PAPER

N₂O decomposition over Cu-ZSM-5 catalysts prepared by the solid-state ion exchange between NH₄-ZSM-5 and copper(II) coordination polymer

Maged S. Al-Fakeh, [ID] *[ab] Bahaa M. Abu-Zied,[b] Aref A. M. Aly[b] and Mahmoud A. Ghandour[b]

The second non-CO_2 greenhouse gas mentioned under the Kyoto Protocol of the United Nations Convention on Climate Change (December 1997) was N_2O. According to this protocol, the European Union, Canada, and Japan were committed to reducing their collective greenhouse gas (GHG) emissions by slightly more than 5 percent below their 1990 levels. Developed countries, also, we are asked to reduce our GHG emissions to at least 5 percent of the 1990 levels, and this is to be achieved till 2012. Since in many situations, N_2O formation is inevitable in the applied processes, catalysts offer a route to N_2O abatement. Over the past several years, more articles have been released that have tried to propose paths through which reduction can be achieved. Nitrous oxide emission, one of the suggested solutions, involves the direct catalytic decomposition of N_2O into its elements. Transition metal exchange zeolites, such as Cu-ZSM-5, Co-ZSM-5, and Fe-ZSM-5, have been reported to exhibit high catalytic activity towards N_2O direct decomposition. This study focused on the activity of a series of Cu-ZSM-5 catalysts, with copper exchange levels of 10–150%, for nitrous oxide (N_2O) decomposition. Different Cu-ZSM-5 catalysts were prepared by applying the solid state ion exchange (SSIE) method through the interaction between NH₄-ZSM-5 and the copper(II) complex. Thermal events emerged during the heat treatment, from ambient temperature to 700 °C, of the two precursors, which were followed by thermal analyses, *viz.* TGA and DTA. Based on the obtained thermal analysis profiles, different mixtures containing NH₄-ZSM-5 and copper(II) coordination polymers were calcined at 550 °C for 3 h in a static air atmosphere. Various integrated physicochemical techniques were used in the characterization of the obtained Cu-ZSM-5 catalysts, including XRD, FT-IR spectroscopy, SEM, N_2-adsorption and electrical conductivity analyses. It was found that the suggested preparation route led to the formation of Cu-ZSM-5, where no CuO or reaction precursors were detected in the 550 °C calcined samples. However, the crystallinity of the obtained Cu-ZSM-5 catalysts was found to decrease with the copper exchange level. The activity of the different Cu-ZSM-5 catalysts was tested for N_2O decomposition in the temperature range of 150–500 °C. The highest activity was exhibited by the catalyst with a copper exchange level of 75%.

1. Introduction

Coordination compounds span the scientific disciplines of organic/inorganic chemistry, biology, materials science, electrochemistry, and pharmacology, with numerous possible applications.[1] N_2O has been gaining momentum as an air pollutant since it is known to increase the greenhouse effect and depletion of the ozone layer in the stratosphere,[2] and this growth seems to have been perpetuated primarily by human activity. Some anthropogenic sources of N_2O are the adipic acid manufacturing to Nylon 6,6,12 to produce nitric acid, fossil fuels, biomass burning, and land use.[3] Decomposing nitrous oxide into its elements, *i.e.* nitrogen and oxygen, is one of the

possible solutions to reduce N_2O emissions. Metal-exchanged zeolites are among the various types of catalysts tested and display desirable activity characteristics in the decomposition of N_2O. This is not merely in the direct decomposition[4–7] and the SCR of N_2O but also in the SCR of NO[10] and the N_2O decomposition with the help of NO.[4,6,11] Some of the tested cations included Co-, Cu-, Fe-, and Rh-containing zeolites, which displayed the best activities, though the structures of the zeolites studied were MFI, MOR, FER and USY zeolites.[8,9] Cu-zeolites have been studied in detail since the finding by Iwamoto *et al.*,[12] in which highly active over-exchanged Cu-ZSM-5 zeolites are active in the decomposition of NO to N_2 and O_2. In addition, N_2O direct decomposition using CuZSM-5 is high.[6] Cu-MOR and Cu-FER zeolite catalysts have also been reported to exhibit good N_2O direct decomposition and NO-assisted N_2O decomposition activities.[6] X-zeolite is a member of the faujasite

ᵃFaculty of Applied Sciences, Taiz University, Taiz 12372, Yemen

ᵇChemistry Department, Faculty of Science, Assiut University, 71516 Assiut, Egypt

(FAU) family with a three-dimensional pore structure and a 12-member ring with a pore diameter of 0.74 nm. X-zeolite is also employed in ion exchange[14] and gas separation and purification because of its high cation content, large pore volume and stable crystal structure.[13] Numerous attempts have been made to establish an effective and repeatable technique for creating high-quality X-zeolite membranes.[15] Many catalytic systems have been investigated, including supported noble metals,[16] calcined hydrotalcites,[17] pure and mixed oxides,[18] and metal-exchanged zeolites.[19] The active sites are mainly found in the internal channels and one on the external surface of the zeolite crystallites in calcined metal-exchanged zeolites.[20] In this paper, we prepared a novel Cu-ZSM-5 catalyst by applying the SSIE method from NH_4-ZSM-5 with a copper(II) coordination polymer[21,22] and used it to decompose nitrous oxide. The catalytic performance of Cu-ZSM-5-75 for N_2O decomposition compares favorably with that of previously reported Cu-based zeolite catalysts. Under similar reaction conditions, Cu-ZSM-5 systems reported in the literature typically achieve high N_2O conversion only at elevated temperatures (>450–500 °C), with activity strongly dependent on copper loading and speciation. In this study, Cu-ZSM-5-75 exhibits enhanced N_2O conversion at comparatively lower temperatures, indicating a higher intrinsic activity associated with the optimized copper exchange level. When normalized per catalyst mass, the observed activity is comparable to or exceeds that reported for conventional Cu-ZSM-5 and Cu-aluminosilicate catalysts prepared by ion exchange or impregnation. Although direct turnover frequency comparisons are challenging due to differences in copper site quantification and reporting methodologies, the high conversion achieved over Cu-ZSM-5-75 suggests efficient utilization of catalytically active copper sites. Furthermore, the catalyst demonstrates stable performance during time-on-stream experiments, consistent with the robustness reported for Cu-exchanged zeolites under N_2O decomposition conditions.[23,24]

2.   Experimental

2.1.   Synthesis of ZSM-5

NH_4-ZSM-5 zeolite, Si/Al ratio 11.4 (SM 27), was purchased from ALSI Penta Zeolite GmbH (Germany). The parent zeolite was subjected to 550 °C for three hours in a static air atmosphere to convert the ammonium form of zeolite into the hydrogen form.

2.2.   Preparation of Cu-ZSM-5 zeolite catalysts

A series of copper-exchanged ZSM-5 zeolite catalysts with the general formula Cu-ZSM-5-x, where x = 10%, 25%, 50%, 75%, 100% and 150%, were prepared by mixing 2 g of zeolite with 0.057, 0.144, 0.289, 0.433, 0.578, and 0.867 g, respectively, of $\{[Cu(DPP)Cl_2(H_2O)_2] \cdot 4H_2O\}_n$ complex in an agate mortar for 30 minutes. Subsequently, the various mixtures were subjected to calcination. In a 3 h period, the temperature was increased to 550 °C and allowed to remain at this temperature for 6 h in air. In this heating process, ion exchange occurs between the copper cations of the complex and the NH_4^+ ions of the zeolite. Then,

the product was allowed to cool to ambient temperature in the room.

3.   Results and discussion

3.1.   FT-IR spectra

Fig. 1 depicts the FT-IR spectra of the H-ZSM-5 and the different Cu-ZSM-5 catalysts being prepared by the calcination of NH_4-ZSM-5 and $[Cu(DPP)(Cl_2)(H_2O)_2] \cdot 4H_2O$ + NH_4-ZSM-5 mixtures, respectively. The IR spectra of ZSM-5 zeolite have been reported by a huge number of authors.[24] As a rule, the internal vibrations of $(Si,Al)O_4$ are vibrational modes close to 1100, 800, and 450 cm^{-1} in ZSM-5 and can also be observed in silica, quartz, and cristobalite.[25,26] By examining the FT-IR spectra of the samples in the frequency range 400–1400 cm^{-1}, it can be observed that all the obtained spectra, Fig. 1, reveal the presence of absorptions at 447, 550, 782, 1072, and 1218 cm^{-1}. Moreover, all samples show the absence of any absorptions at 620 cm^{-1}, which corresponds to the characteristic vibration of cristobalite.[26] According to several authors, absorption bands at around 1072, 782, and 447 cm^{-1} refer to asymmetric, symmetric, and T–O bending vibrations of the internal tetrahedral of ZSM-5, respectively.[23,24] These bands are considered structure insensitive since they appear in the IR-spectra of silica and zeolites, as mentioned before. External asymmetric and double five ring (D5R) vibrations of the ZSM-5 structure of SiO_4 and AlO_4 tetrahedra were observed at 1218 and 550 cm^{-1}, respectively. The characteristics of these zeolites are double five-ring containing zeolites, such as ZSM-5, and hence structure sensitive.[23,24] No peaks characterizing the copper-containing
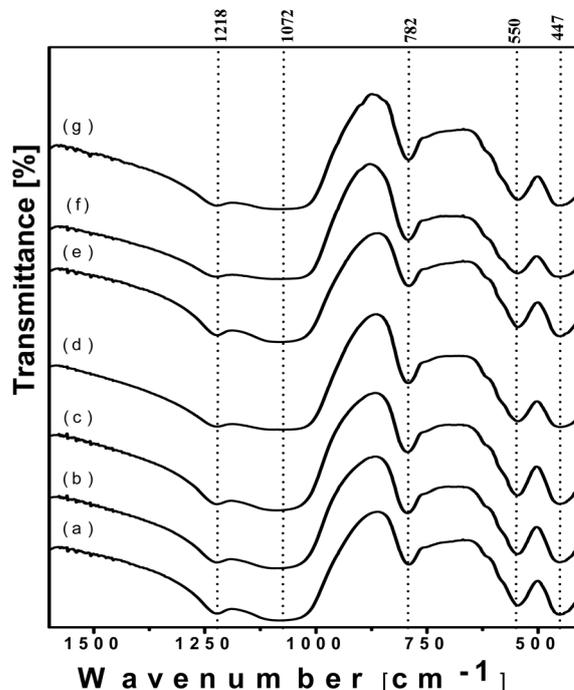

Fig. 1   FTIR spectra obtained for the calcined pure NH_4-ZSM-5 (a) and the different Cu-ZSM-5 catalysts with copper exchange levels of 10% (b), 25% (c), 50% (d), 75% (e), 100% (f) and 150% (g).

complex were detected. Moreover, all the Cu-containing samples (spectra (b–g), Fig. 1) reveal the absence of any absorption bands at 628 and 591 cm^{-1}, which are associated with Cu–O vibrations in bulk CuO.[27] These observations are in good agreement with the DTG analysis and XRD. Particularly, the evidence of Cu-ZSM-5 zeolite formation comes from the disappearance of all the modes due to the Cu-complex, the absence of any absorption due to CuO, and the persistence of those due to the MFI framework in the spectra of all the obtained samples for the SSIE reaction carried out at 500 °C. The optical density obtained by the ratio A_{550}/A_{450} (where A_{550} and A_{450} are the absorbance values at 550 and 450 cm^{-1}, respectively) is normally used to represent the crystallinity of the sample. For the well-crystallized ZSM-5 zeolite, an optical density close to 0.7 was reported by Göhlich et al.[24] The computed optical density values for the neat ZSM-5 and the Cu-ZSM-5 samples with exchange levels of 10%, 25%, 50%, 75%, 100%, and 150% were 0.743, 0.734, 0.728, 0.719, 0.713, 0.708 and 0.704. These values suggest a slight crystallinity decrease with copper loading increase, which is in agreement with the XRD results. Concurrently, P. J. Smeets, et al.[23] reported, based on optical density analysis, that for Bi-ZSM-5 samples, a crystallinity decrease occurs when the Bi content increases.

3.2. Thermal analyses

Fig. 2 shows the TG–DTG and DTA curves of (1,3-di(4-pyridyl) propaneto)(diaqua)(chloro)copper(II)forth-hydrate $\{[Cu(DPP)(Cl_2)(H_2O)_2]\cdot 4H_2O\}_n$ and NH_4-ZSM-5 (ammonium ZSM-5) is a zeolite with an MFI framework in which the negative charge of the aluminosilicate lattice is balanced by ammonium ion (NH_4^+) mixture with a copper exchange level of 75%. A number of steps can be monitored when heating the dried precursor at an ambient temperature of up to 700 °C (Fig. 2). The initial WL step, which begins at ambient temperature until approximately 170 °C, yields a WL percent of about 3. The DTG curve shows a maximum WL step of 213 °C, with a corresponding 2.7 WL percentage. The third WL step is not

a straightforward step; however, it is a compound step with two maxima at 301 and 412 °C (DTG curve), and in total, WL is 13.5%. Our thermal analysis data for the neat complex demonstrated that it decomposes in two steps: the first one extends from 160 to 390 °C, while the second one extends from 410 to 680 °C. Combining this information and the observed thermal events in Fig. 2 suggests the following assignments: (i) the early WL, maximized at 50 °C, could be related to the dehydration of the ZSM-5 zeolite, (ii) the second WL step could be related to the start of complex decomposition, and (iii) the final WL could be ascribed to the second step of the complex decomposition, the ammonia evolution from ZSM-5 zeolite, and the Cu-ZSM-5 formation. In this context, it is worth mentioning that the presence of the ZSM-5 zeolite shifts the temperature of the maximum decomposition of the copper complex towards a lower temperature. This, in turn, suggests the catalytic role of the added zeolite during complex decomposition.

Close inspection of the DTA thermogram obtained for the $[Cu(DPP)(Cl_2)(H_2O)_2]\cdot 4H_2O$ and NH_4-ZSM-5 mixture, Fig. 2, reveals the presence of a small endothermic effect at 206 °C, which is followed by smaller endothermic events. All these effects can be correlated with the start of the complex decomposition. One can clearly observe a sharp exothermic effect maximized at 415 °C. At such a temperature, we could expect two opposing thermal effects: (i) endothermic effects, which are attributable to the complex decomposition and ammonia evolution from the zeolite, and (ii) exothermic effects, which are attributed to the combustion of the evolved gases. From the detection of only an exothermic effect at 415 °C, one can state safely that the exothermic effect predominates.

Fig. 3 shows the weight loss (TG) and the associated derivative thermogram (DTG) of the calcined H-ZSM-5 and Cu-ZSM-5 (75%) in an air atmosphere as a carrier gas. One can easily see that both samples behave similarly; they show a WL profile that extends from ambient till ~600 °C with a total WL% of 12–13%. Such profiles are characteristics for the removal of zeolitic water molecules. Both samples lose most of this water (~10%) till 300 °C with T_{max} of 63–65 °C (DTG curves). This finding suggests that the obtained Cu-ZSM-5 catalysts have hydrophilicity similar to that of the parent H-ZSM-5.
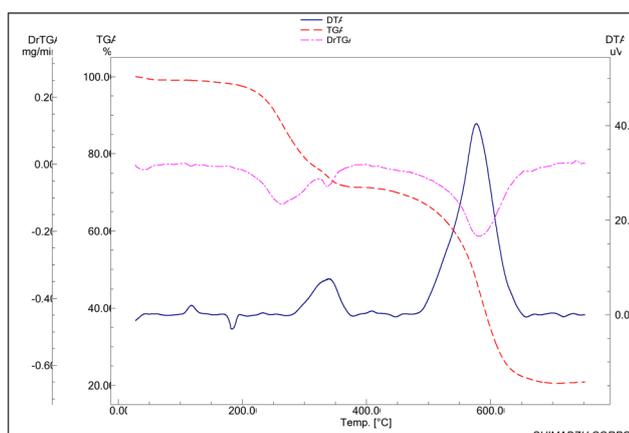

Fig. 2 TG, DTG and DTA thermograms of $\{[Cu(DPP)Cl_2(H_2O)_2]\cdot 4H_2O\}_n$ and NH_4-ZSM-5 in dynamic air.
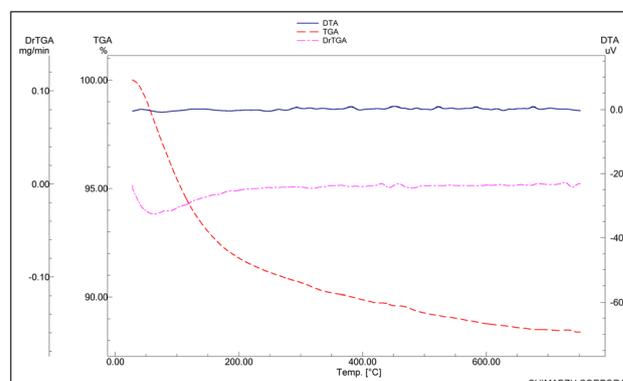

Fig. 3 TG, DTG and DTA thermograms of the calcined H-ZSM-5 and Cu-ZSM-5 (75%) in dynamic air.

3.3. X-ray powder diffraction

Zeolites prepared by applying the SSIE method were analyzed using XRD. The XRD patterns of H-ZSM-5 and those of Cu-ZSM-5 at various exchange levels of copper(II) loading are plotted, as depicted in Fig. 4. The diffraction patterns of the Cu-ZSM-5 samples exhibited two resolved peaks at $2\theta = 7.8°$ and $8.8°$ and three other high intensity reflections at $2\theta = 23°–25°$. These reflections were similar to those in the parent H-ZSM-5 pattern (Fig. 4(a)), corresponding to the ZSM-5 zeolite (MFI structure type).[28] No impurities or major structural changes were detected after copper incorporation. Moreover, no peaks attributable to the CuO phase at $2\theta = 35.6°$ and $38.7°$ can be observed in various Cu-ZSM-5 catalysts.[29] This observation, in turn, indicates that either the Cu(II) species in such samples could be extremely dispersed within the zeolite channels or out on the surface of the crystallites.[30] It has been reported that low-angle

XRD intensities are particularly sensitive to the presence of any species inside channels.[31] Therefore, the crystallinity of the Cu-ZSM-5 samples, expressed as the % of crystallinity, was calculated using the intensity of the reflection at $2\theta = 7.8°$ in the XRD diffractograms. The obtained values are listed in Table 1. On comparing the XRD patterns of the different Cu-ZSM-5 samples as well as the data in Table 1, one can see that the intensity of the diffraction maxima at low angles decreases as a result of increasing the copper(II) content in the zeolite. The gradual reduction in crystallinity of zeolite samples after the incorporation of copper may be because of the possible destruction of some of the frameworks during the process of synthesis owing to the large size of copper(II) in comparison to that of H ones. A similar argument was suggested during the preparation of Ce-ZSM-5.[32]

3.4. Scanning electron microscopy

Most zeolites exhibit different crystalline shapes, such as ellipsoidal, cubic, allied platelets, and coffin-shape (hexagonal prismatic crystals).[33] Fig. 5(a) shows the scanning electron micrograph of the H-ZSM-5 zeolite. Inspection of this photograph revealed that this sample consisted of allied platelets with various crystal sizes. The SEM image of Cu-ZSM-5-75 (Fig. 5(b)) reveals the disappearance of the spherical morphology characterizing the parent Cu-containing complex. The morphology of the Cu-ZSM-5-75 sample shows a similar aggregate to that observed in the neat H-ZSM-5. This indicates that (i) copper incorporation did not induce any changes in the morphology of the ZSM-5 and that (ii) the high dispersion of copper species in the zeolite was revealed by the XRD analysis.

3.5. Nitrogen adsorption

Nitrogen adsorption isotherms, measured at -196 °C, of the standard H-ZSM-5 sample and the Cu-containing ones are shown in Fig. 6. From these isotherms, it is possible to calculate the BET surface area (S_{BET}), the micropore surface area (S_μ), the external surface area ($S_{Ext.}$), and the micropore volume (V_μ) for each sample. The obtained values are listed in Table 1. Inspection of Fig. 6 reveals that the isotherm of the H-ZSM-5 sample belongs to type I of IUPAC classification at low P/P_0 values with some type II features at higher P/P_0 values.[34] All the
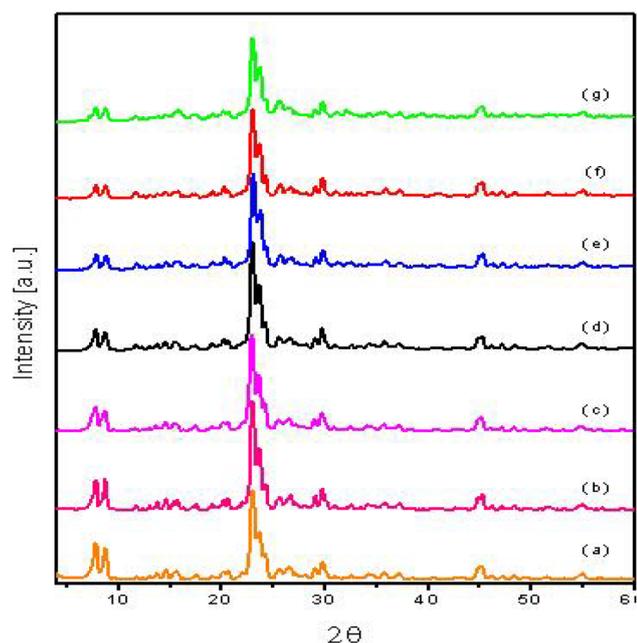

Fig. 4 XRD diffractograms obtained for the calcined pure NH4-ZSM-5 (a) and the different Cu-ZSM-5 catalysts with copper exchange levels of 10% (b), 25% (c), 50% (d), 75% (e), 100% (f) and 150% (g).

Table 1 Degree of crystallinity, textural characteristics, and activation energy of conductivity of different zeolite samples

E_σ [kJ mol^{-1}]	$V_\mu{}^e$ [cm^3 g^{-1}]	$S_{Ext.}{}^d$ [m^2 g^{-1}]	$S_\mu{}^c$ [m^2 g^{-1}]	$S_{BET}{}^b$ [m^2 g^{-1}]	Crystallinity^a [%]	Cu-exchange level [%]
81.31	0.080	110	161	271	100	0
104.06	0.094	88	190	278	89	10
98.28	0.095	84	192	276	72	25
98.08	0.090	94	180	275	68	50
92.53	0.040	169	62	231	52	75
91.09	0.059	123	106	229	49	100
89.23	0.054	27	109	136	48	150

^{a} Crystallinity calculated using the X-ray diffraction patterns. ^{b} S_{BET} is the BET surface area obtained from nitrogen adsorption isotherms in the P/P_0 range of 0.0025–0.30. ^{c} S_μ is the micropore surface area obtained from the t-plot method. ^{d} $S_{Ext.}$ is the external surface area obtained from the t-plot method. ^{e} V_μ is the micropore volume calculated using the t-plot method.
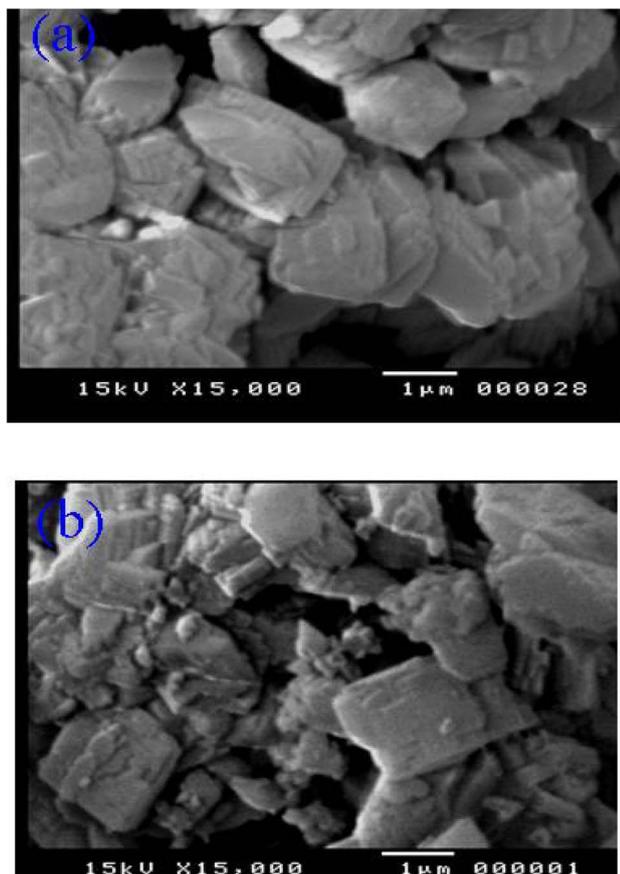
Fig. 5 SEM micrographs of the H-ZSM-5 (a) and Cu-ZSM-5-75 samples (b).

Cu-ZSM-5 samples possess type I isotherms, indicating the microporous nature of these samples, as indicated by the sharp knees at P/P_0 lower than 0.1 due to the filling of micropores. Hysteresis loops of all the samples are close to the low-pressure range in the isotherm of all samples. The loops observed are almost of type H4. The closure point of these loops is approximately at $P/P_0 = 0.1$, which, in turn, suggests the presence of either a strong affinity of adsorbate towards the surface or the existence of ultra-micropores.[35]

As depicted in Fig. 6, increasing the Cu-content is accompanied by a significant lower N_2 adsorption amount at both intermediate and high relative pressure, indicating surface areas decrease as the exchange level increases. The surface areas were computed by applying the BET equation in its linear range of relative pressure 0.0025–0.30; good linearity was obtained with correlation coefficients exceeding 0.99 for all samples. The obtained values are listed in the third column in Table 1. The H-form sample, prepared by direct calcination of the parent NH_4-ZSM-5, shows a BET surface area of 271 $m^2\ g^{-1}$. A slightly higher S_{BET} value, 278 $m^2\ g^{-1}$, is exhibited by Cu-ZSM-5 with an exchange level of 10%. Increasing the Cu-exchange level until 150% is accompanied by a continuous decrease in the relevant S_{BET} values. This observed S_{BET} decrease goes parallel to the gradual crystallinity obtained during the Cu-exchange increase. In this regard, Kharitonov et al.[36] reported
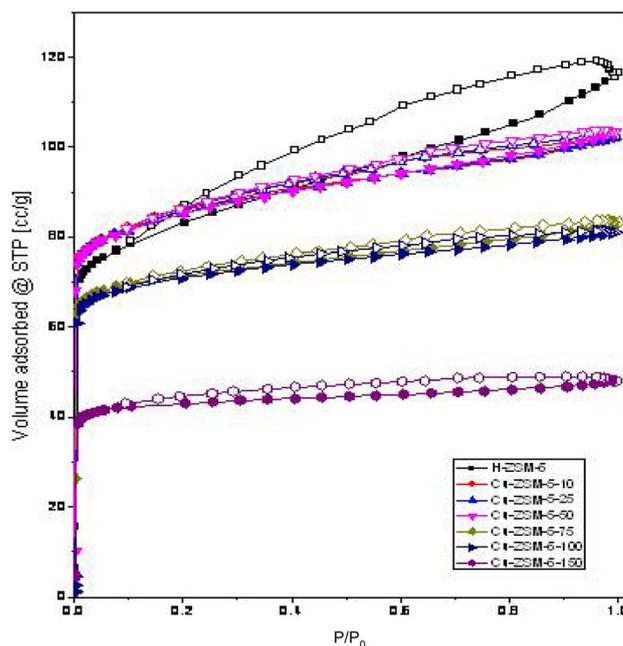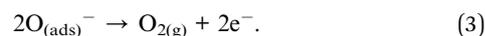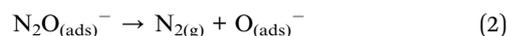

Fig. 6 Nitrogen adsorption (closed symbols)–desorption (open symbols) isotherms of H-ZSM-5 and the various Cu-ZSM-5 samples.

a gradual S_{BET} decrease of Fe-ZSM-5 catalysts accompanying the crystallinity loss, which results from the ball milling effect.

The porous features of the H-ZSM-5 and Cu-ZSM-5 samples were investigated by employing de Bore's t-method.[34] The V_a–t plots of these samples are shown in Fig. 7. From the inspection of this figure, it appears that all the samples exhibit only a negative (downward) deviation, which suggests the microporosity nature of these samples. N_2-physisorption data offer a clear decrease in micropore volume for the samples with a copper exchange level >50%. It can be assumed that the reason for the microporosity could be due to (i) the occlusion of the micropores with some copper containing species and (ii) the observed crystallinity loss, which implies the presence of some amorphous materials that may also block some micropores. Interestingly, the Cu-ZSM-5-75 sample exhibits the highest external surface area and the lowest micropore volume. This large external surface area may be helpful in the reaction of N_2O, resulting in the higher catalytic activity of this sample (vide infra).

The dissociative electron transfer mechanism of N_2O decomposition involves the following steps:

$$N_2O_{(g)} + e^- \rightarrow N_2O_{(ads)}^- \tag{1}$$

$$N_2O_{(ads)}^- \rightarrow N_{2(g)} + O_{(ads)}^- \tag{2}$$

$$2O_{(ads)}^- \rightarrow O_{2(g)} + 2e^-. \tag{3}$$

3.6. Electrical conductivity measurements

The measurements of the electrical conductivity were conducted at the temperature range of 200–500 °C in an air
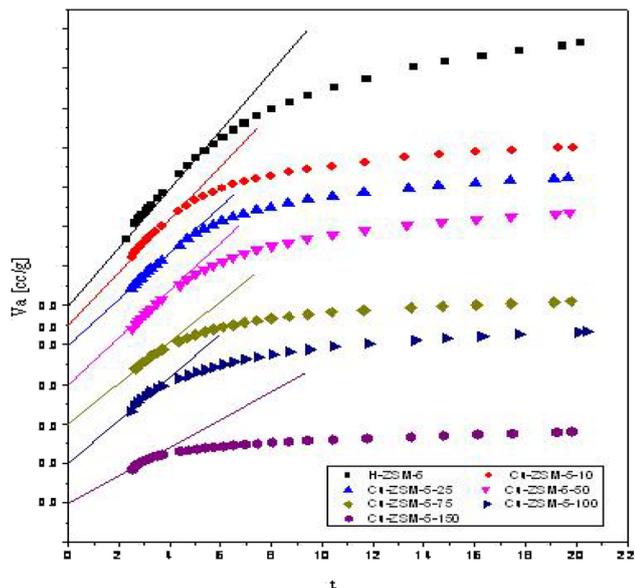
Fig. 7 $V_a - t$ plots of H-ZSM-5 and the various Cu-ZSM-5 samples.

atmosphere for H-ZSM-5 and the various Cu-ZSM-5 catalysts. The obtained results are depicted in Fig. 8. The H-ZSM-5 sample is characterized by a specific conductivity value of 5.26×10^{-6} Ω^{-1} cm^{-1}. This value showed a noticeable increase upon the introduction of copper, *i.e.* for Cu-ZSM-5, at a 10% exchange level. For further increase in the copper content, *i.e.* exchange level, continuous lowering of conductivity is evident. A similar trend of conductivity change with copper exchange level can be observed for lower temperatures (Fig. 8). Ion conduction in zeolites is ascribed to the migration of the exchangeable cations, H$^+$ and/or Cu^{++} ions in our case, along the channels and cavities of the zeolite framework according to an ion-hopping mechanism.[37] It has been reported that such movement is controlled by three factors. The first factor is the electrostatic interaction between these ions and the negatively charged
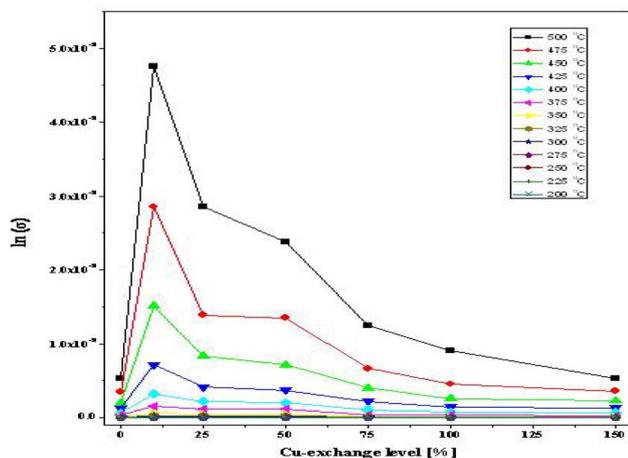
framework of the zeolite, while the second factor is the ratio of the size of these cations to the narrowest points in the channel system. The third factor is the inter-cationic repulsions caused by large ions and high ionic concentrations.[37] The combination of the electrical conductivity measurement results with those of the catalyst characterization suggests that the higher conductivity of the Cu-ZSM-5-10 sample is due to the introduction of copper ions. However, the continuous decrease in conductivity for the samples having copper exchange level ≥25% could be attributed to the gradual crystallinity loss as a result of increasing the copper exchange level. This loss of crystallinity causes the reduction of negative charges per unit volume of the zeolite structure and increases the distance between negative charges. This increment in distance could result in a longer route of cations in the ion-hopping mechanism, consequently leading to a reduction in charge carrier mobility.

In addition, the inter-cationic repulsions caused by the copper ions at high ionic concentrations could be another factor for decreasing the electrical conductivity in the samples having an exchange level of 25% or higher. The activation energies of conductance, E_σ, were calculated by employing the Arrhenius equation, *i.e.* by plotting the $(\ln \sigma)$ against the reciprocal absolute temperature. Good linearity, with an absence of inflection points. The calculated activation energy of conductance values for H-ZSM-5 and the different Cu-ZSM-5 samples follows a trend similar to that observed for the variation of conductivity values with the copper exchange level. The obtained ΔE_a^* values ranged from 81.3 to 104.06 kJ mol^{-1}. These data are in good agreement with those reported for Cu–X zeolites.[38]

3.7. Nitrous oxide decomposition

The catalytic activity of H-ZSM-5, as well as its Cu(II) containing catalysts, was tested towards nitrous oxide direct decomposition. Fig. 9 shows the dependence of the steady-state conversion of N$_2$O on the copper exchange level for the different Cu-ZSM-5 catalysts at elevated catalyst bed temperatures. Three points could be raised from the inspection of Fig. 9: (i) the onset of the reaction starts at temperatures higher than 250 °C over all catalysts; concomitantly, the rate of the reaction increases as the temperature of the reactor increases; (ii) each of the copper bearing catalysts is more active in comparison with H-ZSM-5 at all temperatures of the reactor; and (iii) the activity increases with Cu-content increasing till exchange level reached 75%, maximum N$_2$O decomposition activity 75% at 500 °C, then it shows slight decrease with further Cu-content increase.

In agreement, it was demonstrated that increasing the exchange level until 150% results in an increase in activity for N$_2$O direct decomposition over Cu-ZSM-5 and Co-ZSM-5 being prepared by the conventional ion-exchange from aqueous solutions or using the SSIE method.[5] Based on this literature data and with the aid of the experimental results obtained, it is plausible to suggest that when the activity is expressed as conversion%, we are dealing with two competing effects: (i) positive effect, which is the copper content, *i.e.* the exchange level, and (ii) negative effect, which shows that the crystallinity
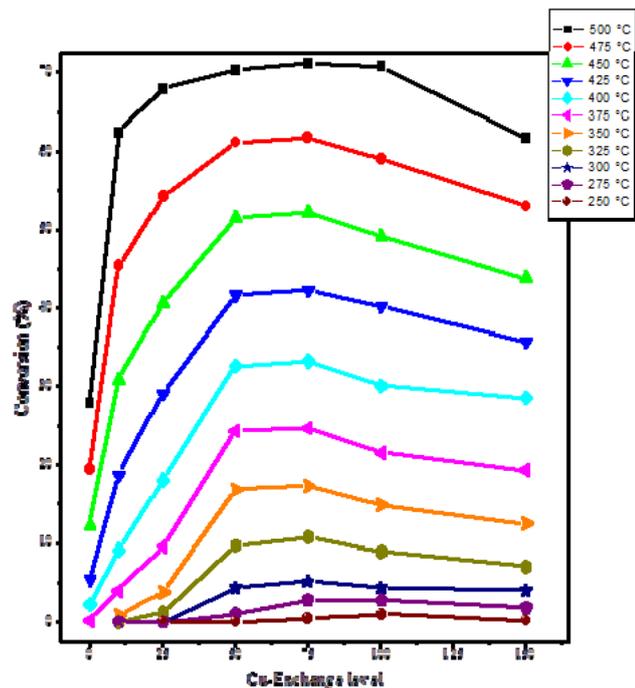

Fig. 8 Variation of $\ln \sigma$ of H-ZSM-5 and the various Cu-ZSM-5 catalysts with exchange levels at different temperatures.

Fig. 9 Dependence of N$_2$O conversion% on the copper exchange level at different reaction temperatures over exchanged ZSM-5 zeolite catalysts as well as the parent H-ZSM-5.

Fig. 10 Dependence of N$_2$O TOFs on the Cu-exchange level for the different Cu-ZSM-5 catalysts. (O = 500 °C, P = 475 °C, Q = 450 °C, R = 425 °C, S = 400 °C, and U = 350 °C.)

loss accompanying the copper content increases. It seems that the Cu-ZSM-5-75 sample exhibits an optimum balance between these two factors.

Another activity picture can be obtained when the activity is expressed in terms of turnover frequencies (TOFs). The TOF is defined as the number of moles of N$_2$O converted per mole of copper per second per square meter of the different Cu-ZSM-5 catalysts. The obtained values are plotted as a function of the Cu-exchange level at different reactor temperatures, as depicted in Fig. 10. It is obvious that the calculated TOFs decrease as the Cu-exchange level increases. Two points could be raised in this respect: (i) this behavior is similar to that observed for the electrical conductivity change over the different Cu-ZSM-5 catalysts (Fig. 8), (ii) this trend of variation is similar to that reported during N$_2$O decomposition over Cu–X zeolite catalysts,[38] and (iii) the obtained TOFs are close to those reported over Cu-ZSM-5 catalysts (prepared by the SSIE method reported between NH$_4$-ZSM-5 and CuCl$_2$)[5] and much higher than those reported over Cu–X catalysts (prepared *via* conventional ion exchange from solution).[38]

The N$_2$O abatement of a family of transition metal exchanged ZSM-5, which was prepared using the SSIE method, was split into two categories: (i) the former has better activity than H-ZSM-5 that contains Co-, Cu-, Fe-, Pd-, Ag-, Ce- and La-ZSM-5 catalysts and (ii) the latter contains Ni-, Y-, Mn-, Zn-, and Cd-ZSM-5 catalysts, with lower activity than H-ZSM-5.[5] It was through *in situ* electrical conductivity measurements that the superiority of the first group catalysts over the second group catalysts was attributed to the fact that the first group catalysts had a higher capacity to be reduced during the heat pre-
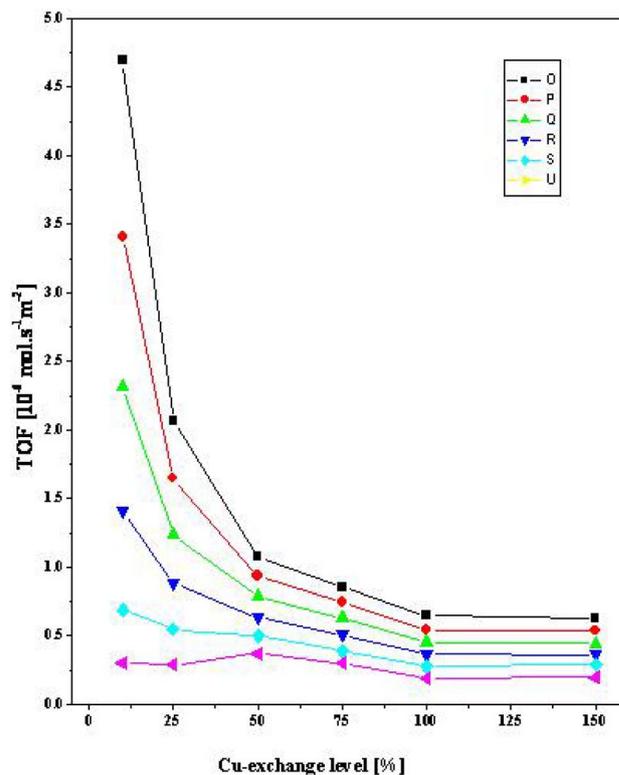
treatment.[5] A similar argument was used during the discussion of the N$_2$O decomposition activity of Cu–X catalysts.[36] Accordingly, from the combination of the data presented in Fig. 8 and 10, we can suggest that besides the influence of structural changes accompanying the Cu-exchange level increase, the catalyst's activity could also be related to their electrical properties, where the ease with which electron transportation from the catalyst bulk to its surface seems to be of great importance in determining the extent of the adsorption process.

The compensation effect has frequently been observed in heterogeneous catalysis.[39] This effect shows a linear relationship between ln A (where A is the pre-exponential factor) and the activation energy (E_a):

$$\ln A = mE_a + c. \quad (4)$$

In cases where a reaction is being studied using different catalysts or in a situation where a series of reactions are being studied using the same catalyst.[39] The behavior of compensation is present during heterogeneous catalysis as well as in homogeneous reactions.[39] This broad phenomenon must support the supposition that the compensation effect is a unitary phenomenon with a general mechanistic background, which extends to the entire field of chemistry and not just to heterogeneous catalysis.[40] Of the particular explanations of this effect, the most commonly discussed include (i) an active surface, (ii) linear correlations between the enthalpy of

adsorption (ΔH) and adsorption entropy (ΔS), and (iii) variable surface concentrations of active sites.[39] Hence, it can be observed that this is a family of catalysts whose number of active sites can be adjusted to a different degree by changing the conditions of the synthesis. It is based on this that the catalysts are analyzed in relation to their different groups with regards to the compensation effect.

The rate constants (k) at the temperature range of 375–500 °C during N_2O decomposition over the different Cu-ZSM-5 catalysts were calculated assuming a first-order rate equation:[41]

$$k = -(F/W)\ln(1 - X), \tag{5}$$

X is the rate of the conversion of N_2O, F is the volumetric rate of flow of reactant and W is the catalyst weight. The Arrhenius equation, that is, the slope of the $\ln k$ *vs.* $1/T$ was used to obtain the activation energies, E_a. Fig. 11 shows the $\ln A$ *vs.* E_a plots obtained for the various Cu-ZSM-5 catalysts. One can easily observe good linearity between the $\ln A$ and E_a values of these three sets of catalysts. Besides, a positive Constable correlation is received (case A in the classification of Bond *et al.*[39]). This, in turn, implies that there is a compensation effect between these catalysts. M and C were calculated to be 6.49 mol kJ^{-1} and 31.15 mol kJ^{-1}, respectively. In this regard, it has been suggested that when the catalysts have one Constable plot, they possess an identical type of transition condition (size and form of the active center) and the reaction mechanism.[42] Therefore, the fact that a straight line was attained in Fig. 11 can be used to indicate that the reaction of N_2O decomposition on the various cobalt containing catalysts takes place through the same process, that is, all catalysts of the three sets contain identical active sites albeit in different amounts depending on the exchange level. We can thus attribute to variable concentrations of active sites, likely of Cu$^+$ and Cu^{2+}, various activation energies with the compensation effect. Their concentrations can be modified at a variety of exchange levels.
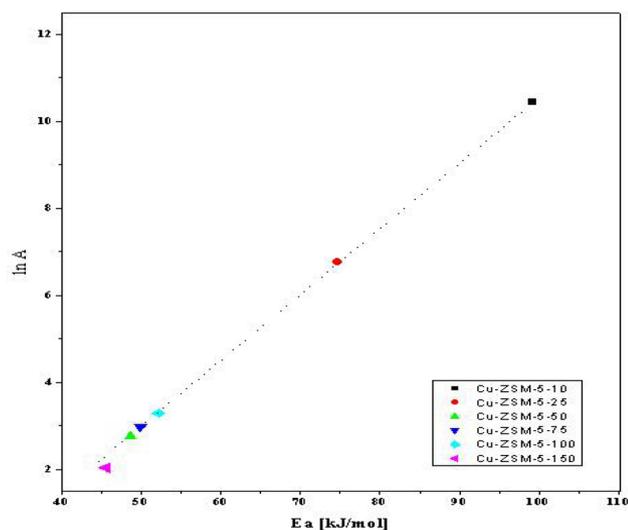

Fig. 11 Compensation relation for N_2O decomposition over the Cu-ZSM-5 catalysts.

4. Conclusion

The following conclusions are derived from our study.

(1) The computed optical density values, calculated from the FT-IR spectra, for the neat ZSM-5 and the Cu-ZSM-5 samples with exchange levels of 10%, 25%, 50%, 75%, 100%, and 150% were found to be 0.743, 0.734, 0.728, 0.719, 0.713, 0.708 and 0.704. These values suggest a slight crystallinity decrease with increasing copper loading, which is in agreement with the XRD data.

(2) All the Cu-ZSM-5 samples possess type I isotherms, indicating the microporous nature of these samples, as indicated by the sharp knees at P/P_0 lower than 0.1 due to the filling of micropores.

(3) Increasing the Cu-content is accompanied by a significant lowering in the amount adsorbed of N_2 gas at both intermediate and high relative pressures, indicating surface areas decrease with the exchange level increasing. Moreover, N_2-physisorption data offer a clear decrease in micropore volume for the samples with a copper exchange level >50%.

(4) Ion conduction in zeolites is ascribed to the migration of the exchangeable cations, H$^+$ and/or Cu^{++} ions in our case, along the channels and cavities of the zeolite framework by a mechanism of ion-hopping.

(5) The catalytic activity of N_2O direct decomposition revealed the following: (i) the onset of the reaction starts at temperatures higher than 250 °C over all catalysts; meanwhile, the activity increases with increasing reactor temperature; (ii) all the Cu^{++} containing catalysts exhibit higher activity, compared to H-ZSM-5 all over the reactor temperatures; and (iii) the activity increases with Cu-content increase till an exchange level of 75% (maximum N_2O decomposition activity of 75% at 500 °C); then, it shows slight decrease on further Cu-content increase.

(6) A good linearity between the $\ln A$ and E_a values was obtained for N_2O decomposition over all the tested catalysts. This, in turn, suggests the existence of a compensation effect among these catalysts, *i.e.* all catalysts of the three sets sharing the same active sites. However, the number of active sites increases and decreases depending on the preparation method. In other words, the catalytic decomposition of N_2O proceeds *via* the same mechanism.

(7) Oxygen evolution was observed over all the Cu-ZSM-5 catalysts during N_2O decomposition reactions. These catalysts showed an activity increase until an exchange level of 75% in the case of N_2O decomposition. At higher exchange levels, a mild activity decrease was observed.

Conflicts of interest

The authors declare no conflicts of interest.

Data availability

The authors confirm that the data supporting the findings of this study are available in the article.

Acknowledgements

References

1 K. Fromm, *Coord. Chem. Rev.*, 2008, **252**, 856.

2 *Climate Change: The Science of Climate Change*, ed. J. T. Houghton, L. G. Meira, B. A. Callander, N. Harris, A. Kattenberg and K. Maskell, Cambridge University Press, Cambridge, 1996.

3 J. Pérez-Ramírez, F. Kapteijn, K. Schöffel and J. A. Moulijn, *Appl. Catal., B*, 2003, **44**, 117–151.

4 L. Li, Q. Shen, J. Li, Z. Hao, Z. P. Xu and G. Q. M. Lu, *Appl. Catal., A*, 2008, **344**, 131–141.

5 B. M. Abu-Zied, W. Schwieger and A. Unger, *Appl. Catal., B*, 2008, **84**, 277–288.

6 P. J. Smeets, M. H. Groothaert, R. M. van Teeffelen, H. Leeman, E. J. M. Hensen and R. A. Schoonheydt, *J. Catal.*, 2007, **245**, 358–368.

7 G. D. Pirngruber, P. K. Roy and R. Prins, *J. Catal.*, 2007, **246**, 147–157.

8 K. Sugawara, T. Nobukawa, M. Yoshida, Y. Sato, K. Okumura, K. Tomishige and K. Kunimori, *Appl. Catal., B*, 2007, **69**, 154–163.

9 M. N. Debbagh, A. Bueno-López, C. S. Martínez de Lecea and J. Pérez-Ramírez, *Appl. Catal., A*, 2007, **327**, 66–72.

10 Y. Kuroda and M. Iwamoto, *Top. Catal.*, 2004, **28**, 111.

11 M. Kögel, B. M. Abu-Zied, M. Schwefer and T. Turek, *Catal. Commun.*, 2001, **2**, 273–276.

12 M. Iwamoto, H. Yahiro, K. Tanda, N. Mizuno, Y. Mine and S. Kagawa, *J. Phys. Chem.*, 1991, **95**, 3727.

13 F. Benaliouche, Y. Boucheffa, P. Ayrault, S. Mignard and P. Magnoux, *Microporous Mesoporous Mater.*, 2008, **111**, 80–88.

14 U. D. Joshi, P. N. Joshi, S. S. Tamhankar, V. V. Joshi, C. V. Rode and V. P. Shiralkar, *Appl. Catal., A*, 2003, **239**, 209–220.

15 X. Yin, G. Zhu, Z. Wang, N. Yue and S. Qiu, *Microporous Mesoporous Mater.*, 2007, **105**, 156–162.

16 J. Oi, A. Obuchi, A. Ogata, G. R. Bamwenda and K. Mizuno, *Chem. Lett.*, 1995, 453.

17 S. Kannan and C. S. Swamy, *Appl. Catal., B*, 1994, **3**, 109.

18 R. Larsson, *Catal. Today*, 1989, **4**, 235.

19 Y. Li and J. N. Armor, *Appl. Catal., B*, 1992, **1**, L21.

20 E. A. Urquieta-González, L. Martins, R. P. S. Peguin and M. S. Batista, *Mater. Res.*, 2002, **5**, 321.

21 M. S. Al-Fakeh, Synthesis, thermal stability and kinetic studies of copper(II) and cobalt(II) complexes derived from 4-aminobenzohydrazide and 2-mercaptobenzothiazole, *Eur. Chem. Bull.*, 2020, **9**(12), 403–409.

22 A. A. M. Aly, M. S. Al-Fakeh and M. A. Ghandour, Nano-sized metal 1,3-di(4-pyridyl)propane coordination polymer prepared via the surface layer-by-layer chemical deposition method, *Nano Sci. Nano Technol.*, 2014, **8**, 265–273.

23 P. J. Smeets, *et al.*, Direct NO and N_2O decomposition and NO-assisted N_2O decomposition over Cu-zeolites: Elucidating the influence of the CuCu distance on oxygen migration, *J. Catal.*, 2007, **245**(2), 358–368.

24 M. Göhlich, W. Reschetilowski and S. Paasch, Spectroscopic study of phosphorus modified H-ZSM-5, *Microporous Mesoporous Mater.*, 2011, **142**(1), 178–183, DOI: 10.1016/j.micromeso.2010.11.033.

25 T. Xue, Y. M. Wang and M.-Y. He, *Microporous Mesoporous Mater.*, 2012, **156**, 29.

26 K. Kordatos, S. Gavela, A. Ntziouni, K. N. Pistiolas, A. Kyritsi and V. Kasselouri-Rigopoulou, *Microporous Mesoporous Mater.*, 2008, **115**, 189.

27 M. M. Mohamed, *J. Colloid Interface Sci.*, 2003, **265**, 106.

28 M. M. Treacy, J. B. Higgins and R. Von Ballmoos, *Collection of Simulated XRD Powder Patterns for Zeolites*, Elsevier, New York, 3rd rev. edn, 1996.

29 C. Dossi, A. Fusi, S. Recchia, R. Psaro and G. Moretti, *Microporous Mesoporous Mater.*, 1999, **30**, 165.

30 A. L. Villa, C. A. Caro and C. M. de Correa, *J. Mol. Catal. A: Chem.*, 2005, **228**, 233.

31 D. Dumitriu, R. Bârjega, L. Frunza, D. Macovei, T. Hu, Y. Xie, V. I. Pârvulescu and S. Kaliaguine, *J. Catal.*, 2003, **219**, 337.

32 T. M. Salama, M. M. Mohamed, I. Othman A and G. A. El-Shobaky, *Appl. Catal., A*, 2005, **286**, 85.

33 F. L. Bleken, S. Chavan and B. Louis, *Appl. Catal., A*, 2012, **447**, 178.

34 G. Leofanti, M. Padovan, G. Tozzola and B. Venturelli, *Catal. Today*, 1998, **41**, 207.

35 N. A. Eltekova, D. Berek, I. Novák and F. Belliardo, *Carbon*, 2000, **38**, 373.

36 A. S. Kharitonov, V. B. Fenelonov, T. P. Voskresenskaya, N. A. Rudina, V. V. Molchanov, L. M. Plyasova and G. I. Panov, *Zeolites*, 1995, **15**, 253.

37 G. Kelemen and G. Schön, *J. Mater. Sci.*, 1992, **27**, 6036.

38 B. M. Abu-Zied, *Microporous Mesoporous Mater.*, 2011, **139**, 59.

39 G. C. Bond, M. A. Keane and H. Kral, Compensation phenomena in heterogeneous catalysis: general principles and a possible explanation, *Catal. Rev.*, 2000, **42**(3), 323–383.

40 G. C. Bond, A. D. Hooper, J. C. Slaa and A. O. Taylor, *J. Catal.*, 1996, **163**, 319.

41 B. M. Abu-Zied and A. M. El-Awad, *J. Mol. Catal. A: Chem.*, 2001, **176**, 227.

42 G. C. Bond, *Z. Phys. Chem.*, 1985, **144**, 21.